

CERIUM INCORPORATED INTO A MESOPOROUS MOLECULAR SIEVE (MCM-41)

G. E. do Nascimento*, M. M. M. B. Duarte and C. M. B. M. Barbosa

Departamento de Engenharia Química, Universidade Federal de Pernambuco,
Avenida Artur de Sá, s/n, 50740-521, Recife - PE, Brazil.
Fax: (55) (81) 2126-7278
E-mail: grazielen@yahoo.com.br

(Submitted: February 27, 2014 ; Revised: June 30, 2015 ; Accepted: July 9, 2015)

Abstract - The synthesis and characterization of a mesoporous molecular sieve (MCM-41) was studied due to its high surface area and large pore volume and to target potential applications in adsorption and catalysis. Rare earth elements have special chemical properties and are efficient promoters for supports. In this study, a mesoporous molecular sieve that incorporates the transition metal cerium (Ce-MCM-41) was synthesized using the hydrothermal method with the goal of improving the structural properties for adsorption. The molar composition of the obtained gel was 1CTMABr: 4SiO₂: 1Na₂O: 0.2Ce₂O₃: 200H₂O. The pure mesoporous molecular sieve MCM-41 was also synthesized using the same method. The materials were characterized by the following techniques: XRD, BET/BJH, SEM/EDS, TG and FT-IR. A preliminary test to evaluate the materials as adsorbents to remove naphthenic acids present in jet fuel was performed. The results of the characterization showed that the incorporation of the metal cerium did not affect the MCM-41 structure and that mesoporous materials were formed. Ce-MCM-41 exhibited good thermal stability, high specific surface area and large pore volume, which are characteristics of a good adsorbent. From the preliminary test, the adsorptive capacity increased by 60% with the incorporation of cerium in the MCM-41 structure.

Keywords: Mesoporous molecular sieves; Ce-MCM-41; Synthesis; Characterization.

INTRODUCTION

The mesoporous molecular sieve MCM-41, which is a member of the M41S family, was first discovered by the Mobil Company in 1992 to eliminate diffusion pore restrictions present in zeolites due to its micropores, which limit its use with larger molecules for adsorption and catalytic conversions (Beck *et al.*, 1992; Corma *et al.*, 1997).

Since then, much interest has been focused on their properties and applications due to the hexagonal arrangement, their high specific surface areas, narrow pore size distribution and controllable and wide spectrum of pore diameters (15-100 Å) in the mesoporous region (Jiang *et al.*, 2007; Zhao *et al.*, 2011).

The mesoporous molecular sieves can be applied in areas of catalysis and adsorption, can control pollution in the environment (Hao *et al.*, 2006; Qin *et al.*, 2007; Puangnaga and Unob, 2008) and can be used in technology that employs advanced materials based on molecular sieves, such as electron transfer photosensors, semiconductors, polymers, carbon fibers, clusters and materials with nonlinear optical properties (Beck *et al.*, 1992; Corma *et al.*, 1997; Northcott *et al.*, 2010).

However, the base of the mesoporous molecular sieve is amorphous silica, which contains a considerable number of silanol groups and, due to its neutral character, exhibits limited activities in adsorption and catalysis (Qin *et al.*, 2015). To expand its field of application, improvements are required in

*To whom correspondence should be addressed

This is an extended version of the work presented at the 20th Brazilian Congress of Chemical Engineering, COBEQ-2014, Florianópolis, Brazil.

its synthesis, in which silicon is replaced with other ions. The incorporation of heteroatoms into MCM-41 walls allows one to control its features, which makes it possible to obtain materials with predetermined properties, such as surface acidity, redox properties, basicity and thermal stability (Oliveira *et al.*, 2005; González Vargas *et al.*, 2013).

Molecular sieves can generate more basic or acid sites as desired for the particular application (Li *et al.*, 2010). These active sites are created by isomorphous substitution of silicon by a metal with the goal of improving the adsorptive and catalytic applications. The creation of basic sites on the surface of MCM-41 favors its affinity for acidic compounds, which improves its adsorption capacity. In recent decades, the incorporation of heteroatoms into the MCM-41 structure has been investigated (González Vargas *et al.*, 2013; Li *et al.*, 2013).

The incorporation of transition metals (Nilsen *et al.*, 2007; Anunziata *et al.*, 2008), rare earth metals (Zhao *et al.*, 2011; Akondi *et al.*, 2012) and alkaline earth metals (Wu *et al.*, 2011; Nascimento *et al.*, 2014) into MCM-41 produces new types of adsorbents.

The incorporation of rare earth metals into mesoporous silicates showed an improvement in their thermal stability and structural properties, such as pore volume and surface area, compared with that of pure MCM-41 (Chien *et al.*, 2005).

Given the above discussion, the goal of this study was to investigate the mesoporous molecular sieve MCM-41 incorporating cerium through its synthesis and its characterization. This material can be used as an adsorbent to remove naphthenic acids present in jet fuel.

EXPERIMENTAL

Synthesis of Mesoporous Molecular Sieves MCM-41 and Ce-MCM-41

The mesoporous molecular sieve Ce-MCM-41 was synthesized using the hydrothermal method (Nascimento *et al.*, 2014) with silica gel and sodium silicate as the silicon source, cetyltrimethylammonium bromide (CTMABr) as a structural director, cerium nitrate as a transition metal source and distilled water. The synthesis was conducted at 100 °C in a Teflon-jacketed stainless steel autoclave for a period of five days with a daily correction pH range of 9.5-10.0 with a 30% solution of acetic acid. The molar composition of the gel obtained was 1CTMABr: 4SiO₂: 1Na₂O: 0.2Ce₂O₃: 200H₂O. Then, the obtained mate-

rial was subjected to a calcination process using a heating ramp of 5 °C min⁻¹, beginning from ambient temperature to 500 °C, in an inert atmosphere of nitrogen at a flow rate of 100 mL min⁻¹, which remained in this condition for 1 hour. Then, the flow was exchanged with synthetic air at a rate of 100 mL min⁻¹ for an additional period of 1 hour.

The pure mesoporous molecular sieve MCM-41 was also synthesized by the same method.

Characterization of Mesoporous Molecular Sieve MCM-41 and Ce-MCM-41

The characterization of the materials was performed using X-ray diffraction (XRD); N₂ adsorption/desorption by the BET and BJH method; scanning electron microscopy with energy dispersive spectroscopy (SEM/EDS); thermogravimetric analysis (TG) and Fourier transform infrared (FT-IR) spectroscopy.

X-ray diffraction measurements were performed on a BRUKER D8 ADVANCE diffractometer using Cu-K α radiation. N₂ adsorption and desorption were obtained using an ASAP 2420 from MICROMERIT-ICS. The spectrum energy dispersive X-ray and electron microscopy of the sample scan were obtained in an energy dispersive spectrometer coupled to a scanning electron microscope (Shimadzu Superscan SS-550) using 15 V. The TG curve was obtained in a thermobalance (NETZSCH STA 449 F3 Jupiter model) in an atmosphere of 100 mL min⁻¹ of nitrogen. The absorption spectra in the infrared region were obtained with an infrared absorption spectrometer VERTEX 70 of BRUKER using KBr as a dispersing agent.

Preliminary Test

n-Dodecanoic acid (C₁₂H₂₄O₂) (99% purity, Merck) was used as the model adsorbate to represent naphthenic acids and n-dodecane (C₁₂H₂₆) (99% purity, Merck) as the solvent.

The experiment was performed in a finite bath system while stirring at 300 rpm using a shaker table (IKA brand, KS 130C model). Assays were performed at ambient laboratory temperature (25 °C \pm 2 °C), and blanks were conducted using the same procedure. A 50-mL Erlenmeyer flask containing 0.05 g of sorbent and 5 mL of the model mixture with a known initial concentration of 1 wt.% n-dodecanoic acid was used. Aliquots were removed at periods of 10, 30, 60, 120, 240, 300, 360, 420 and 480 min.

RESULTS AND DISCUSSION

Characterization of Mesoporous Molecular Sieves MCM-41 and Ce-MCM-41

X-Ray Diffraction (XRD): Figure 1 shows the X-ray diffractograms of the synthesized MCM-41 and Ce-MCM-41 samples after calcination.

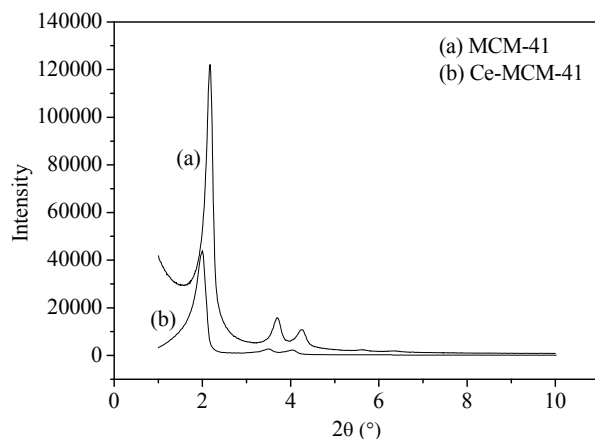


Figure 1: X-ray diffraction after calcination of MCM-41 (a) and Ce-MCM-41 (b).

It can be observed from Figure 1 that the synthesized MCM-41 and Ce-MCM-41 materials showed an X-ray pattern similar to that shown in the literature for mesoporous materials (Beck *et al.*, 1992).

The X-ray diffraction pattern of MCM-41 showed the presence of a strong diffraction peak (100) at $2\theta = 2.17^\circ$ and two low intensity peaks at (110) and (200) of 3.69° and 4.27° , which indicates the formation of orderly mesoporous material. The X-ray diffraction pattern of Ce-MCM-41 also showed the presence of these peaks at (100), (110) and (200) $2\theta = 2.00^\circ$, 3.48° and 4.04° , respectively, which indicates that the structure of hexagonal MCM-41 was maintained after introducing cerium into its structure. There was also a decrease in the relative intensity of the diffraction patterns of Ce-MCM-41 in comparison with MCM-41, which indicates the inclusion of cerium according to Subhan *et al.* (2012), Bing *et al.* (2012; 2013) and Akondi *et al.* (2014).

The unit cell parameter (a_0) was calculated using the formula $a_0 = 2d_{100}/\sqrt{3}$, and the value of the d-spacing (d_{100}) was obtained from the XRD pattern peak using the Bragg equation ($2d \sin\theta = \lambda$, where $\lambda = 1.5406$ for Cu-K α). Table 1 shows these parameters for the MCM-41 and Ce-MCM-41 materials after calcination.

Table 1: The cell parameters, pore diameter, pore volume, pore wall and surface area of MCM-41 and Ce-MCM-41.

Sample	d_{100} (nm)	a_0 (nm)	S_{BET} ($m^2 g^{-1}$)	Pore diameter (nm) ^a	Pore volume ($cm^3 g^{-1}$)	Pore wall (nm) ^b
MCM-41	4.07	4.70	908.7	3.96	0.84	0.74
Ce-MCM-41	4.41	5.09	756.8	4.43	0.76	0.66

^aPore diameter obtained from BJH analysis of desorption data.

^bPore wall = a_0 - pore diameter.

Table 1 shows that the values of a_0 and d_{100} increased after the incorporation of cerium, which is due to the substitution of Si^{4+} ions by Ce^{4+} ions, which are larger (Bing *et al.*, 2012; González Vargas *et al.*, 2013).

N₂ adsorption/desorption by BET and BJH method: N₂ adsorptions/desorptions of MCM-41 and Ce-MCM-41 after calcinations are shown in Figure 2.

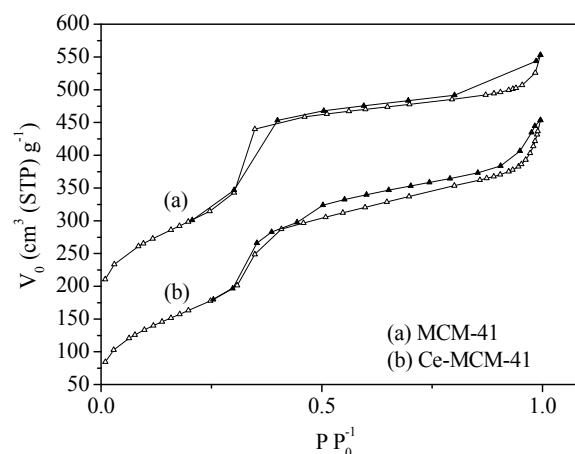


Figure 2: Isotherms of N₂ adsorption/desorption of MCM-41 (a) and Ce-MCM-41 (b) after calcination. Δ Adsorption and \blacktriangle Desorption.

As shown in Figure 2 and based on the classification of the International Union of Pure and Applied Chemistry (IUPAC), the isotherms of N₂ adsorption/desorption of both materials exhibited type IV behavior typical of mesoporous materials (IUPAC, 1982). The isotherms showed a sharp upturn in the relative pressure range of 0.3-0.4, which is due to capillary condensation of nitrogen into the pores (Akondi *et al.*, 2014).

The pore diameter, pore volume, pore wall and surface area of MCM-41 and Ce-MCM-41 after calcination are shown in Table 1. The results show that the surface area, pore volume and pore wall decreased when cerium was added to the MCM-41 structure. This can be attributed to the existence of

cerium in the channels of MCM-41. Also, there was an increase in the unit cell parameters and pore diameter, which can be attributed to the Ce atomic size (radius = 1.01 Å) being larger than that of Si (radius = 0.54 Å), which corroborates the XRD results. These results are consistent with reports of other authors (Chien *et al.*, 2005; Bing *et al.*, 2012, 2013; González Vargas *et al.*, 2013; Akondi *et al.*, 2014).

The MCM-41 and Ce-MCM-41 materials showed a high specific surface area and large pore volume, which is a prerequisite for their potential applications as adsorbents.

Scanning electron microscopy with energy dispersive spectroscopy (SEM/EDS): The electron micrographic scans of the MCM-41 and Ce-MCM-41 materials that were calcined at 500 °C are shown in Figure 3.

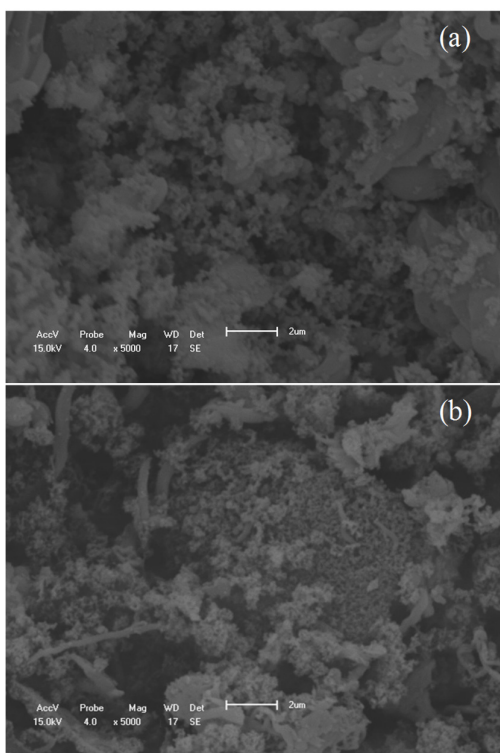


Figure 3: MCM-41 (a) and Ce-MCM-41 (b) micrographs.

From Figure 3, it can be observed that tubular grains were formed in both materials. The samples had hexagonal or spherical micelle-like edged rods. Similar micrographs were also obtained by Chien *et al.* (2005), Park *et al.* (2007), Akondi *et al.* (2012) and Bing *et al.* (2013).

The energy dispersive X-ray spectra of these materials are shown in Figure 4.

The energy dispersive spectroscopy (EDS) spec-

tra of MCM-41 in Figure 4 show that the structure of the synthesized material was pure silica. The presence of cerium was observed in Ce-MCM-41 because the EDS spectrum contained a characteristic peak, which confirmed the presence of this element in the same mesoporous structure. Peaks due to silicon appeared with higher intensity, followed by oxygen, which are constituents of the mesoporous material. In addition, peaks related to the presence of gold and carbon were observed due to the metallization process through which the sample passed.

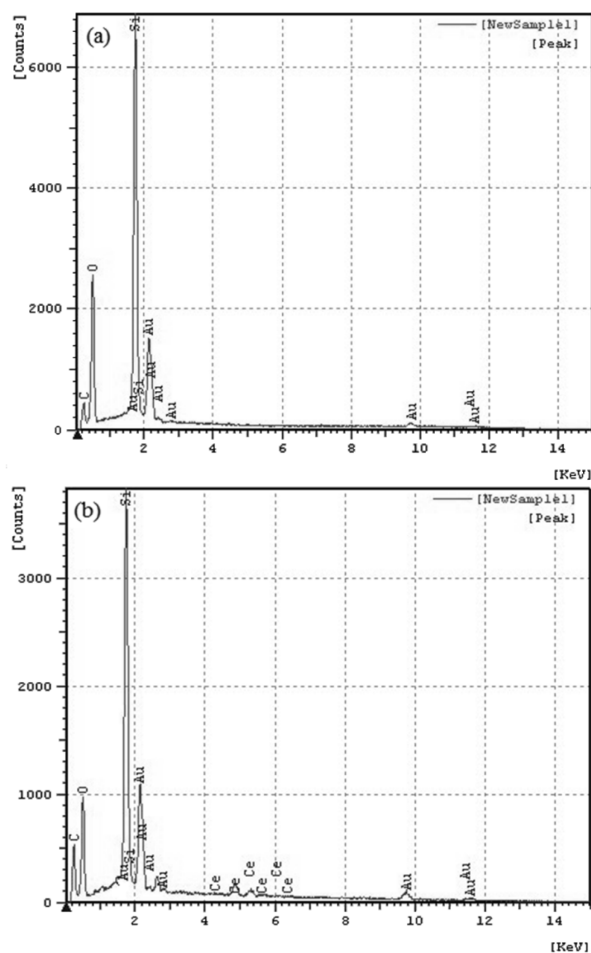


Figure 4: MCM-41 (a) and Ce-MCM-41 (b) EDS spectra.

Thermal analysis (TG): The curves from the thermogravimetric analysis (TG) for the MCM-41 and Ce-MCM-41 samples that were not calcined are shown in Figure 5.

Figure 5 shows that both materials experienced three distinct regions of mass loss. The first mass loss was attributed to physically adsorbed water desorption (below 200 °C). The second mass loss, between 200 and 500 °C, was due to the decomposition

and combustion of the organic director. After decomposition of the surfactant, the material continued to lose mass, which is related to water loss from the condensation of silanol groups at the inner surface of the pores with the driver interacting molecules. This region is in the range above 600 °C. These results were also observed by Zhao *et al.* (2011), who synthesized MCM-41 incorporating europium.

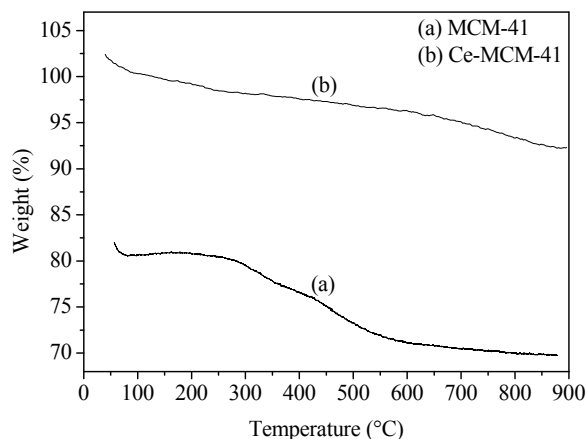


Figure 5: Thermogravimetric curves for MCM-41 (a) and Ce-MCM-41 (b).

Ce-MCM-41 exhibited a higher thermal stability with a residual weight of 92% at 900 °C, whereas MCM-41 had a residual weight of 70%. The modification of the MCM-41 silica framework with the rare earth metal caused an increase in the thermal stability of the material, which may improve its adsorption capacity.

Spectroscopy in the Fourier transform infrared (FT-IR) region: Infrared spectra of Ce-MCM-41 before and after calcinations are shown in Figure 6.

The infrared spectra of the MCM-41 and Ce-MCM-41 samples before and after calcination showed bands in the region of 500-4000 cm^{-1} , which are characteristic of the fundamental vibration of the MCM-41 network in accordance with the literature (Akondi *et al.*, 2012).

The absorption bands at approximately 3400 cm^{-1} and 1650 cm^{-1} were observed in both the MCM-41 and Ce-MCM-41 materials, which correspond to stretching of the O-H bond of water and water adsorbed at the surface. Absorption bands at approximately 1250, 1080 and 800 cm^{-1} refer to the asymmetric and symmetric stretching of the Si-O-Si bond network. MCM-41 shows no vibration at 960 cm^{-1} , and a new band appeared at 970 cm^{-1} in the spectrum of Ce-MCM-41, which is attributed to the stretching of the bond Si-O-M (M = Ce). This result indicates the presence of cerium in the structure. These bands

were also observed by Park *et al.* (2007), Subhan *et al.* (2012), González Vargas *et al.* (2013) and Akondi *et al.* (2014) in their studies.

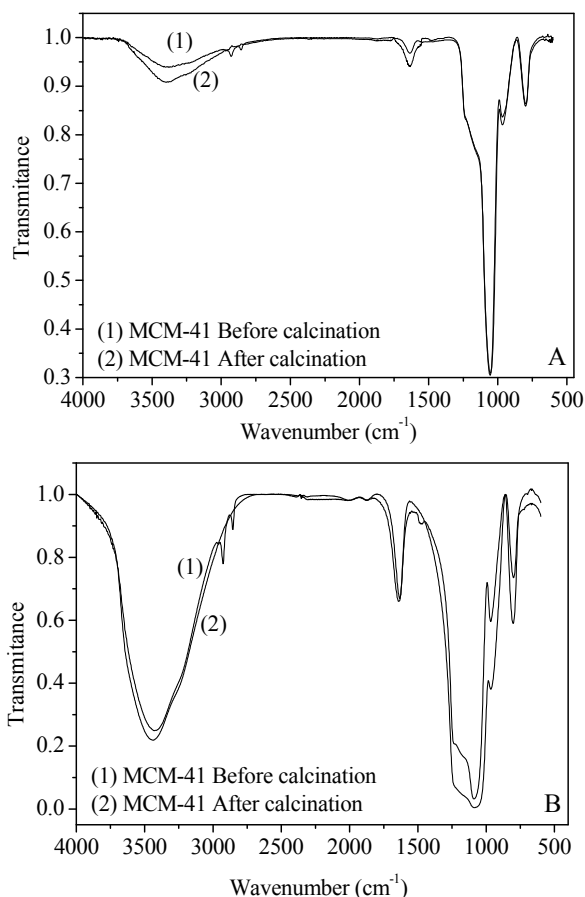


Figure 6: FT-IR spectra of MCM-41(A) and Ce-MCM-41(B) before (1) and after (2) calcination.

In both the MCM-41 and Ce-MCM-41 samples, the presence of the template could be confirmed by the bands in the 2800-2900 cm^{-1} region that are related to C-H stretching. After calcination, these bands of the directing agent disappeared, which indicates that the calcination process was effective in removing such a compound, which was also observed by Park *et al.* (2007) and Nascimento *et al.* (2014). This result corroborates those found in the thermal analysis when there was mass loss due to the removal of the structure directing agent.

Both MCM-41 and Ce-MCM-41 materials showed functional groups that positively influence the adsorption of specific substances.

Preliminary Test

The progress of naphthenic acid adsorption, which is represented by the model mixture of n-

dodecanoic acid in n-dodecane when using the adsorbents MCM-41 and Ce-MCM-41, is presented in Figure 7.

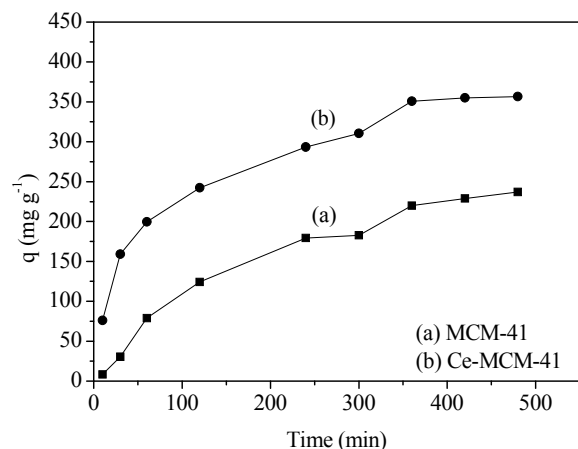


Figure 7: Preliminary test of naphthenic acid adsorption by the adsorbents (a) MCM-41 and (b) Ce-MCM-41. Ratio = 0.01 (mass of adsorbent/solution volume) and agitation = 300 rpm.

It was observed that the incorporation of cerium into the MCM-41 structure promoted an average increase in the adsorptive capacity of approximately 60%.

These results highlight the importance of the incorporation of the rare earth metal cerium into the mesoporous materials for obtaining a greater removal of naphthenic acids by adsorption.

CONCLUSION

The method of synthesis used to obtain the adsorbent Ce-MCM-41 was effective because mesoporous material was formed, and the incorporation of cerium metal did not affect the structure of MCM-41, which was verified by the results obtained in the characterization of the material. The material showed good thermal stability, high specific surface area and a large pore volume. The adsorbent showed technical potential to remove naphthenic acids present in jet fuel.

ACKNOWLEDGMENT

PRH-28, ANP, PETROBRÁS, UFPE and CETENE for analysis and characterization of the material.

REFERENCES

- Akondi, A. M., Trivedia, R., Sreedhara, B., Kantam, M. L. and Bhargava, S., Cerium-containing MCM-41 catalyst for selective oxidative arene cross-dehydrogenative coupling reactions. *Catal. Today*, 198, 35 (2012).
- Akondi, A. M., Kantam, M. L., Trivedi, R., Sreedhar, B., Buddana, S. K., Prakasham, R. S. and Bhargava, S., Formation of benzoxanthenones and benzochromenones viacerium-impregnated-MCM-41 catalyzed, solvent-free, three-component reaction and their biological evaluation as anti-microbial agents. *J. Mol. Catal. A: Chem.*, 386, 49 (2014).
- Anunziata, O. A., Beltramone, A. R. and Cussa, J., Synthesis at atmospheric pressure and characterization of highly ordered Al, V, and Ti-MCM-41 mesostructured catalysts. *Catal. Today*, 133, 891 (2008).
- Beck, J. S., Vartuli, J. C., Roth, W. J., Leonowicz, M. E., Kresge, C. T. and Schmitt, K. D., A new family of mesoporous molecular sieves prepared with liquid crystal templates. *J. Am. Chem. Soc.*, 114, 10834 (1992).
- Bing, J., Li, L., Lan, B., Liao, G., Zeng, J., Zhang, Q. and Xukai Li, X., Synthesis of cerium-doped MCM-41 for ozonation of p-chlorobenzoic acid in aqueous solution. *Appl. Catal. B - Environ.*, 115, 16 (2012).
- Bing, J., Wang, X., Lan, B., Liao, G., Zhang, Q. and Li, L., Characterization and reactivity of cerium loaded MCM-41 for p-chlorobenzoic acid mineralization with ozone. *Sep. Purif. Technol.*, 118, 479 (2013).
- Chien, S., Kuo, M. and Chen, C., Synthesis, characterization and catalysis of Ce-MCM-41. *J. Chin. Chem. Soc.*, 52, 733 (2005).
- Corma, A., Kan, Q., Navarro, M. T., Pariente, J. P. and Rey, F., Synthesis of MCM-41 with different pore diameters without addition of auxiliary organics. *Chem. Mat.*, 9, 2124 (1997).
- González Vargas, O. A., De Los Reyes Heredia, J. A., Montesinos Castellanos, A., Chen, L. F. and Wang, J. A., Cerium incorporating into MCM-41 mesoporous materials for CO oxidation. *Mater. Chem. Phys.*, 139, 125 (2013).
- Hao, X.-Y., Zhang, Y.-Q., Wang, J.-W., Zhou, W., Zhang, C. and Liu, S., A novel approach to prepare MCM-41 supported CuO catalyst with high metal loading and dispersion. *Microporous Mesoporous Mater.*, 88, 38 (2006).
- International Union of Pure and Applied Chemistry (IUPAC). Reporting Physisorption Data for Gas/Solid Systems, 54, 2201 (1982).

- Jiang, T. S., Zhao, Q. and Yin, H. B., Synthesis of highly stabilized mesoporous molecular sieves using natural clay as raw material. *Appl. Clay Sci.*, 35, 155 (2007).
- Li, D., Min, H., Jiang, X., Ran, X., Zou, L. and Fan, J., One-pot synthesis of Aluminum-containing ordered mesoporous silica MCM-41 using coal fly ash for phosphate adsorption. *J. Colloid Interface Sci.*, 404, 42 (2013).
- Li, X., Li, B., Xu, J., Wang, Q., Pang, X., Gao, X., Zhou, Z. and Piao, J., Synthesis and characterization of Ln-ZSM-5/MCM-41 (Ln=La, Ce) by using kaolin as raw material. *Appl. Clay Sci.*, 50, 81 (2010).
- Nascimento, G. E., Duarte, M. M. M. B., Schuler, A. R. P. and Barbosa, C. M. B. M., Synthesis, characterization, and application of the mesoporous molecular sieve Sr-MCM-41 in the removal of naphthenic acids from a model mixture of aviation kerosene by adsorption. *Brazilian Journal of Petroleum and Gas*, 8(1), 1 (2014).
- Nilsen, M. H., Antonakou, E., Bouzga, A., Lappas, A., Mathisen, K. and Stocker, M., Investigation of the effect of metal sites in Me-Al-MCM-41 (Me = Fe, Cu or Zn) on the catalytic behavior during the pyrolysis of wooden based biomass. *Microporous Mesoporous Mater.*, 105, 189 (2007).
- Northcott, K. A., Miyakawa, K., Oshima, S., Komatsu, Y., Perera, J. M. and Stevens, G. W., The adsorption of divalent metal cations on mesoporous silicate MCM-41. *Chem. Eng. J.*, 157, 25 (2010).
- Oliveira, A. C., Range, M. C., Fierro, J. L. G., Reyes, P. and Oportus, M., Efeito do Cromo nas Propriedades Catalíticas da MCM-41. *Quim. Nova*, 28, 37 (2005). (In Portuguese).
- Park, S. H., Kim, B. H., Selvaraj, M. and Lee, T. G., Synthesis and characterization of mesoporous Ce-Mn-MCM-41 molecular sieves. *J. Ind. Eng. Chem.*, 13, 637 (2007).
- Puangnana, M. and Unob, F., Preparation and use of chemically modified MCM-41 and silica gel as selective adsorbents for Hg (II) ions. *J. Hazard. Mater.*, 154, 578 (2008).
- Qin, J., Li, B., Zhang, W., Lv, W., Han, C., Liu, J., Synthesis, characterization and catalytic performance of well-ordered mesoporous Ni-MCM-41 with high nickel content. *Microporous Mesoporous Mater.*, 208, 181 (2015).
- Qin, Q., Ma, J. and Liu, K., Adsorption of nitrobenzene from aqueous solution by MCM-41. *J. Colloid Interface Sci.*, 315, 80 (2007).
- Subhan, F., Liu, B. S., Zhang, Y. and Li, X. G., High desulfurization characteristic of lanthanum loaded mesoporous MCM-41 sorbents for diesel fuel. *Fuel Process Technol.*, 97, 71 (2012).
- Wu, G., Jiang, S., Li, L. and Guan, N., Nitridation of BaO supported on mesoporous materials: Basicity characterization and catalytic properties. *Appl. Catal., A*, 391, 225 (2011).
- Zhao, Q., Wang, G. W., Wu, D. L., Zhou, X. P. and Jiang, T. S., Microwave synthesis and textural property of europium substituted mesoporous molecular sieves. *J. Phys. Chem. Solids*, 72, 34 (2011).